

This is a repository copy of *Investigating the association between solar flares and the complexity of sunspot groups and their asymmetric behavior*.

White Rose Research Online URL for this paper: https://eprints.whiterose.ac.uk/id/eprint/232841/

Version: Accepted Version

Article:

Tirnakci, M., Chowdhury, P., Kilcik, A. et al. (2 more authors) (2025) Investigating the association between solar flares and the complexity of sunspot groups and their asymmetric behavior. Advances in Space Research. ISSN: 0273-1177

https://doi.org/10.1016/j.asr.2025.09.094

© 2025 The Authors. Except as otherwise noted, this author-accepted version of a journal article published in Advances in Space Research is made available via the University of Sheffield Research Publications and Copyright Policy under the terms of the Creative Commons Attribution 4.0 International License (CC-BY 4.0), which permits unrestricted use, distribution and reproduction in any medium, provided the original work is properly cited. To view a copy of this licence, visit http://creativecommons.org/licenses/by/4.0/

Reuse

This article is distributed under the terms of the Creative Commons Attribution (CC BY) licence. This licence allows you to distribute, remix, tweak, and build upon the work, even commercially, as long as you credit the authors for the original work. More information and the full terms of the licence here: https://creativecommons.org/licenses/

Takedown

If you consider content in White Rose Research Online to be in breach of UK law, please notify us by emailing eprints@whiterose.ac.uk including the URL of the record and the reason for the withdrawal request.





Available online at www.sciencedirect.com

ScienceDirect

Advances in Space Research xx (2025) xxx-xxx

ADVANCES IN SPACE RESEARCH (a COSPAR publication)

www.elsevier.com/locate/asr

Investigating the Association between Solar Flares and the Complexity of Sunspot Groups and Their Asymmetric Behavior

Melike Tirnakci^{a,b}, Partha Chowdhury^c, Ali Kilcik^{a,*}, Jean-Pierre Rozelot^d, Robertus Erdelyi^{e,f,g}

^aDepartment of Space Science and Technologies, Akdeniz University Faculty of Science, 07058, Antalya, Türkiye
^bTürkiye National Observatories, TUG, 07070, Antalya, Türkiye

^cUniversity College of Science and Technology, Chemical Technology Dept., University of Calcutta, 92, Acharya Prafulla Chandra Road, Kolkata, 700009, India ^dUniversité de la Côte d'Azur (emeritus), 77 chemin des basses moulières, Grasse, 06130, France

^eSolar Physics and Space Plasma Research Centre, School of Mathematical and Physical Sciences, University of Sheffield, Hicks Building, Hounsfield Road, Sheffield, S3 7RH, United Kingdom

^fBay Zoltán Solar Observatory (GSO), Hungarian Solar Physics Foundation (HSPF), Gyula Petőfi tér 3, Gyula, H-5700, Hungary
^gDepartment of Astronomy, Eötvös Loránd University, 1/A Pázmány Péter sétány, Budapest, H-1117, Hungary

Received —; Received in final form —; Accepted ——;

Available online ——-

Abstract

Solar activity exhibits a range of quasi-periodic variations among different indices, reflecting the complex dynamics of the Sun. In this study, we investigate the temporal variation and hemispheric asymmetry of sunspot counts (SSC), sunspot areas (SSA), and x-ray solar flares during Solar Cycles 23 (SC23), SC24, and the ascending and maximum phase of SC 25 (1996–2024). We analyzed the flare production potential (FPP) and flare efficiency ratio (FER) using the third parameter of the modified Zurich/McIntosh classification system in different hemispheres. We performed cross-correlation analysis to investigate the time-lagged correlations between SSC, SSA, and solar flare. Notable periodicities such as 27-day solar rotation, about 150-day Rieger-type periods, and quasi-biennial oscillations (QBOs) are detected through multitaper and wavelet spectral analyses. Our main findings are: i) Our findings show that an increase in the complexity of sunspot groups is associated with an increase in FPP and FER. This relationship is consistently observed across different hemispheres and solar cycles. These findings provide further statistical support for using the complexity of sunspot groups as a pre-cursor parameter in models to predict solar flares. ii) The number of statistically significant mid-term periods in the northern hemisphere appears to be fewer compared to the southern hemisphere. While QBOs are present in both hemispheres, their spatial and temporal variations manifest unevenly, with the southern hemisphere exhibiting more prominent and distinct evolutionary patterns, particularly during the studied cycles. iii) The periodic behaviors of SSC, SSA, and x-ray solar flare numbers exhibit distinct dependencies on the investigated cycle phase and hemispheric asymmetries, with variations in amplitude and timing across different solar cycles.

© 2025 COSPAR. Published by Elsevier Ltd All rights reserved.

Keywords: Hemispheric asymmetry; Solar activity; Solar periodicity; Sunspot complexity

1. Introduction

The Sun is our nearest star, having a very complex and dynamic body with different structural layers and these layers have distinct dynamic behaviors. It is found that the magnetic field of the Sun exhibits systematic variations with periods of a few minutes to thousands of years (Usoskin, 2017). The Sun often goes through various non-stationary active processes with the release

Email addresses: meliketirnakci@gmail.com (Melike Tirnakci), alikilcik@akdeniz.edu.tr (Ali Kilcik)

^{*}Corresponding author: Tel.: +0-000-000-0000; fax: +0-000-000-0000;

30

31

of energy across all wavelengths of the electromagnetic spectrum. Several variations in the output energy were observed in many solar activity indicators, such as the sunspot number (SSN), sunspot areas (SSA), Ca–K plages, solar flares/flare index, and 10.7 cm solar radio flux (F10.7). All of these indicators show cyclic behavior with a dominant period of about 11 years (Sunspot/Schwabe cycle).

Apart from the ~11-year solar cycle change, sunspots in the photosphere also exhibit a ~27-day rotational period and ~22-year periodicity (Hale Cycle) for the reversal of global solar magnetic polarity (Hathaway, 2015). These variations of the solar magnetic field modulate different solar energetic events and are one of the major sources influencing space weather (Georgoulis et al., 2024) and the Earth's upper atmosphere (Georgieva & Veretenenko, 2023; Temmer, 2021).

Sunspots emerge on the solar visible disk as dark regions where the magnetic field is concentrated, and therefore the plasma 13 temperature is lower than in the surroundings. Sunspots or solar active regions (ARs) appear in various sizes, shapes, lifetimes, and magnetic complexities/topologies. ARs, according to the structure, distribution of spots in the interior of the group, or the complexity of the sunspot groups (SGs), are classified into three categories known as the McIntosh classification scheme (McIntosh, 1990; McCloskey et al., 2016). According to this classification, the first component is the modified Zurich class (A, B, C, D, E, F, and H), describing the length and the total magnetic flux of the SG; the second component is based on penumbral class (x, r, s, a, h, 18 and k), which narrates the symmetry of the penumbra of the principal spot and the magnetic field topology; and the third component is based on the compactness of the spots (x, o, i, and c) 1. The third component reflects the internal complexity and evolutionary stage of sunspot groups. The classes are ordered x < 0 < i < c in terms of increasing compactness and magnetic complexity. This 21 progression is closely linked to flare productivity as more compact and complex groups (especially those in class 'c') are generally 22 at more advanced stages of evolution and more likely to produce solar flares. The third component of the McIntosh classification 23 improves the classification scheme by measuring the internal compactness of sunspots within a group. While classes D, E, and characterize the evaluated sunspot groups with bipolar structure, the letter "c" provides additional information on the internal 25 magnetic complexity of these groups. This improvement enhances the ability of the classification system to represent both the 26 magnetic complexity and the flare efficiency of sunspot groups (Janssens et al., 2025) 27

On the other hand, solar flares, one of the most explosive solar phenomena, commonly originate within SGs, where the evolution of complex magnetic fields leads to magnetic reconnection and the subsequent release of a huge amount of energy (10^{29} to 10^{32} erg) within a very short time interval (Priest & Forbes, 2002). During this reconnection process, stored magnetic energy is rapidly converted into both thermal and kinetic energy, including the non-thermal acceleration of energetic particles (Shibata & Magara, 2011; Emslie et al., 2012). These large-scale solar eruptive phenomena significantly affect the near-Earth environment, influencing the safety of space-borne satellites and communication systems (Pulkkinen, 2007; Schrijver & Mitchell, 2013; Temmer, 2021; Erdélyi et al., 2022; Korsós et al., 2024).

Solar flares are divided into five classes according to their strength between 0.1 and 0.8 nm spectral bands (soft x-rays) observed by the Geostationary Orbiting Environmental Satellites (GOES). The flare classes, from weak to strong, are A ($< 10^{-7} \text{ W m}^{-2}$), B ($10^{-7} \text{ to } 10^{-6} \text{ W m}^{-2}$), C ($10^{-6} \text{ to } 10^{-5} \text{ W m}^{-2}$), M ($10^{-5} \text{ to } 10^{-4} \text{ W m}^{-2}$), and X ($\ge 10^{-4} \text{ W m}^{-2}$). The first four levels are divided into sub-units from 1 to 9 based on intensity, while the X-class has no upper limit. Major powerful flares are produced from the complex types of SGs like D, E, and F classes in the modified Zurich classification (Sammis et al., 2000; Toriumi et al., 2017; Eren et al., 2017; Kilcik et al., 2018; Gao, 2020).

¹https://www.stce.be/educational/classification

It was reported that different solar activity proxies, like sunspot number, sunspot areas, Ca–K plages, photospheric magnetic flux, and solar flares, exhibit several periodic and quasi-periodic variations between 27 days and 11 years, called "intermediate-term periods." Two well-known examples of these mid-term variations are the Rieger-type periodicities (130–190 days) (Lean & Brueckner, 1989; Oliver et al., 1998; Knaack et al., 2005; McIntosh et al., 2015; Kiss et al., 2017, 2018; Kiss & Erdélyi, 2018; Chowdhury et al., 2022, 2024; Korsós et al., 2023) and the 0.6-4 years (220-1460 days) quasi-biennial oscillations (QBOs) (Akioka et al., 1987; Obridko & Shelting, 2001; Vecchio & Carbone, 2009; Bazilevskaya et al., 2014; Kilcik et al., 2020; Ravindra et al., 2022; Elek et al., 2024).

Several studies demonstrated that different solar activities are asymmetric about the equator (Arlt et al., 2013). This phenomenon, known as the north-south asymmetry of solar activities, is a systematic and real phenomenon (Ataç & Özgüç, 1996; Norton et al., 2014; Kiss et al., 2017; Schüssler & Cameron, 2018; Ravindra et al., 2021; Zhang et al., 2022). The north-south asymmetry of the solar indices also exhibits several intermediate-term quasi-periodicities (Badalyan & Obridko, 2011; Chowdhury et al., 2019; Ravindra et al., 2021).

Solar flares are closely correlated with the evolution of different classes of SGs (Zirin & Liggett, 1987; McIntosh, 1990). Therefore, the association of different classes of SGs with flare production is an important topic to understand the physical link between solar explosive events and the solar magnetic field. It also sheds light on forecasting changes in the near-Earth space weather. Several studies have been carried out to investigate the association of solar flares and SGs (Smith & Howard, 1968; Bornmann & Shaw, 1994; Sammis et al., 2000; Eren et al., 2017; Kilcik et al., 2018; Toriumi & Wang, 2019; Gao, 2020; Lin et al., 2023; Oloketuyi et al., 2023; Li et al., 2024; Korsós et al., 2015, 2020, 2024). In the present work, we investigate the relationship between the soft x-ray flare-production potential and the third component (x, o, i, and c) of the McIntosh classification for the period of 1996–2024, which includes the entire SC23 (1996–2008), SC24 (2009–2019), and a major portion of the rising branch (2020–2024) of the current SC25. We have determined the asymmetric properties and periodic/quasi-periodic behavior of sunspot counts (SSC) and Solar X-class flares for the aforesaid period, along with flare production potential for both hemispheres.

2. Data and Methods

The sunspot number and x-ray solar flare data for the period 1996-2024 used in this study were obtained from the National Oceanic and Atmospheric Administration (NOAA) Space Weather Prediction Centre (SWPC) ². The raw data contains information such as NOAA identification numbers, heliographic coordinates, sunspot area, sunspot count and McIntosh class, x-ray flare class, etc. of observed sunspot groups. To ensure data reliability and minimize projection-related effects, sunspot groups with zero or missing area values and those beyond ±70° heliographic longitude were excluded from the analysis. The data were used to analyze temporal variations and investigate the north-south asymmetry in x-ray solar flare. Note that only C-, M-, and X-class solar flares were considered. In the cross-correlation, multitaper method (MTM; Thomson, 1982; Ghil et al., 2002; Kilcik et al., 2024) and wavelet analysis (Torrence & Compo, 1998), the daily data were used, while monthly data were used for the temporal variation analysis.

The measure of hemispheric asymmetry is defined as follows:

$$Asymmetry = \frac{\text{North} - \text{South}}{\text{North} + \text{South}} \tag{1}$$

²https://www.swpc.noaa.gov/products/solar-region-summary

In this equation, any solar activity indicator could be used. If the result of this equation is negative, it means that the southern hemisphere is dominant (Li et al., 2009; Zhang et al., 2015).

We plotted temporal variations to analyze and compare the north-south asymmetry of SSC and x-ray solar flares. Afterwards, we categorized the x-ray flares into the north and south hemisphere according to the third parameter of the McIntosh classification (x, o, i and c). Then, we calculated the flare production potential for each hemisphere, using the following equation:

$$FPP = \frac{\text{Total number of flaring sunspot groups in a specific class}}{\text{Total number of the same class sunspot groups}}$$
 (2)

Let us also introduce the following quantity, the Flare Efficiency Ratio (FER), to establish how many flares are produced by each flaring active region in these specific groups (x, o, i and c):

$$FER = \frac{\text{Total number of observed flares in a specific class}}{\text{Total number of the same class sunspot groups}}$$
(3)

Furthermore, the errors associated with FPP and FER were estimated using the standard error approach, as both are ratio-based metrics derived from a single parameter. In contrast, for the asymmetry ratio, which depends on two independent parameters (e.g., North and South), we employed an error propagation method based on partial derivatives (Tellinghuisen, 2001). This distinction in error calculation ensures a more accurate representation of uncertainty in each metric.

The cross-correlation analysis was performed to investigate the time-lagged correlations between SSC, SSA, and solar flare, providing insights into their temporal variations, interdependencies, and potential lead-lag relationships. To examine the evolution of solar flare occurrences, sunspot numbers, and sunspot areas, we applied the MTM, which is effective for spectral analysis, allowing us to identify periodicities with high resolution while minimizing spectral leakage. This method utilizes orthogonal windows or tapers to obtain an estimate of the power spectrum (Ghil et al., 2002). The MTM approach provides a robust method for examining the frequency content of data across different time scales, offering valuable tools for spectral estimation (Thomson, 1982) and signal reconstruction (Park, 1992) in a time series that may contain both broadband and line components. In the MTM analysis, we restricted our domain of interest to a frequency range of 0.0004-0.04 (i.e., 25-2500 days). Note that we used the red noise approximation to calculate the confidence levels of the detected periodicities. To improve the interpretation and visualization of the results, the power spectra were normalized based on the 95% confidence level. To do normalization we just divided the power and significance values to the 95% confidence level values. This normalization allowed us to clearly highlight statistically significant peaks across the spectral domain.

We also applied Morlet wavelet analysis, a powerful technique for examining localized changes in periodic patterns within a time series (Lau & Weng, 1995; Torrence & Compo, 1998). The wavelet transform, which forms the basis of this analysis, is given by the following equation:

$$\Psi(t) = \pi^{-1/4} e^{i\omega_0 t} e^{-t^2/2} \tag{4}$$

Here, ω_0 represents the nondimensional frequency and t is the nondimensional time. ω_0 can be set according to the frequency region to be analyzed and the amplitude of the wave is focused in a certain region in time. In this study we set $\omega_0 = 6$, which provides a reasonable temporal and spatial resolution since the wavelet and Fourier interval are related by a factor of 1.03 (Farge, 1992; Torrence & Compo, 1998; Chowdhury & Dwivedi, 2012).

3. Analysis and Results

104

Table 1 presents the rates of hemispheric asymmetry. The negative values suggest predominance of the southern hemisphere in SC23 and SC24. SC25, which has not yet been completed, so far shows the predominance of the southern hemisphere.

112

113

116

117

118

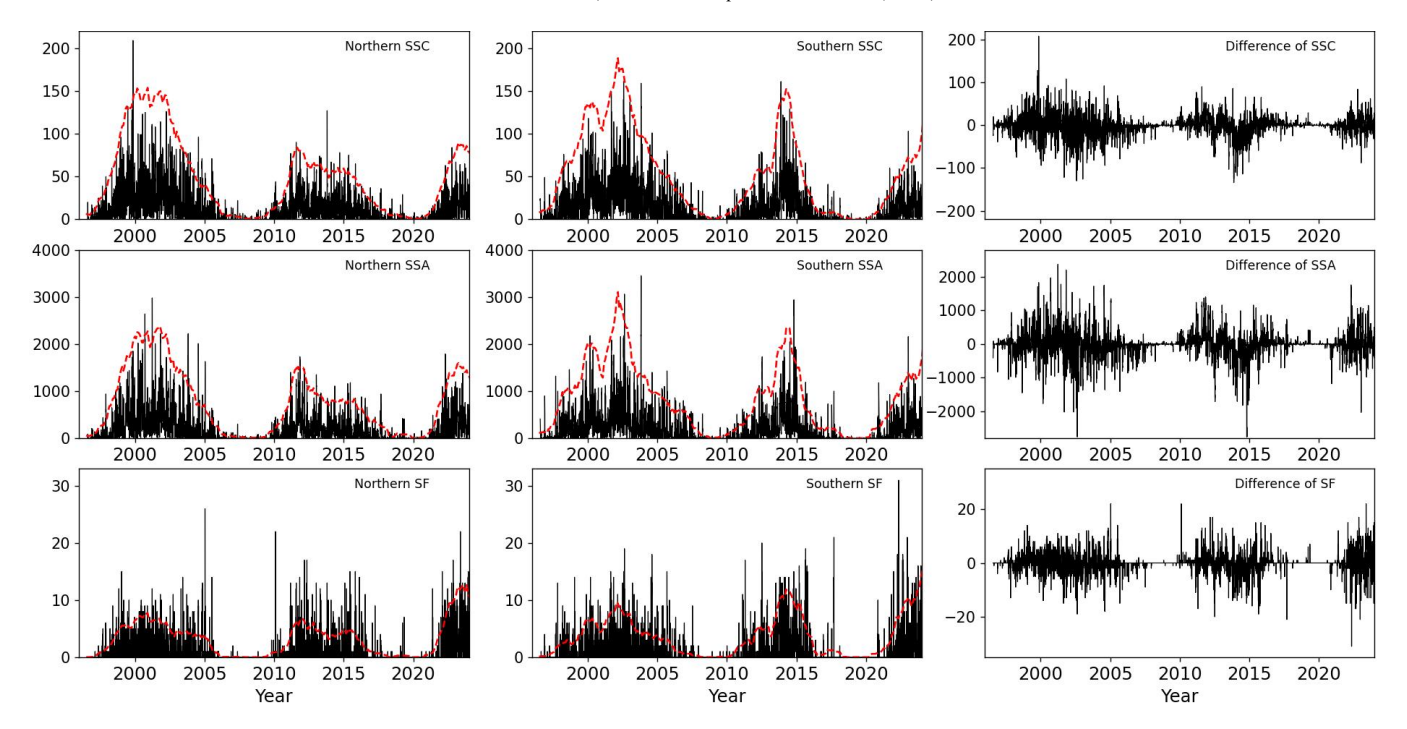


Fig. 1. Temporal variation of sunspot counts (SSC), sunspot area (SSA), and total solar flare numbers for the northern hemisphere (left column) and southern hemisphere (middle column). Black bars show daily values, and red dashed lines represent smoothed trends (the smoothed data were multiplied by four for SSC, SSA and total number of solar flares to clearly visualize the variations). The first row shows total SSC, the second row represents total SSA, and the third row depicts total number of solar flare numbers for each hemisphere. Last column shows the difference in SSC, SSA and total number of solar flares.

Figure 1 shows the variation and hemispheric differences of SSC, SSA, and the number of total solar flares in the northern and southern hemispheres for SC23, SC24 and the ascending and maximum phases of SC25. It is observed that the SSC, SSA and the number of flares in both hemispheres follow the 11-year solar cyclic behavior.

Table 1. Hemispheric Asymmetry Ratio

Cycle	SSC	SSA	Total Flare
23	-0.07 ± 0.003	-0.07 ± 0.001	-0.05 ± 0.012
24	-0.02 ± 0.004	-0.02 ± 0.001	-0.12 ± 0.013
25	-0.17 ± 0.004	-0.15 ± 0.001	-0.17 ± 0.012

In terms of SSC, SSA, and the total number of x-ray solar flares, SC23 exhibits a clear southern hemisphere dominance throughout most of the cycle. While SC24 also shows an overall southern dominance, a short-term enhancement in the northern hemisphere is visible around the first peak, particularly reflected in the smoothed trends shown in the left column of Fig 1. In SC25, the smoothed trends in Figure 1 indicate relatively comparable activity levels between two hemispheres, although the southern hemisphere still maintains a modest dominance across all three parameters. Table 4 shows that 54% of SSCs in SC23, 51% in SC24, and 59% in SC25 occurred in the southern hemisphere.

One noteworthy observation is the difference in the distribution of SSC, SSA, and total flare numbers between the hemispheres. In SC23 and SC24, the northern hemisphere shows a wide distribution of these metrics throughout the cycle. In contrast, during SC24, the southern hemisphere exhibits a piling up of SSC, SSA, and total flare numbers, particularly concentrated around the cycle maximum. To explain this "piling up" in SC24, 44% of SSCs in the northern hemisphere and 70% in the southern hemisphere (each calculation is relative to their respective hemisphere during the cycle) occurred between 2013 and 2015. Similar patterns are observed in the SSA and total number of solar flares, with 39% and 47% in the northern hemisphere, 68% and 70% in the southern

hemisphere during the same period, respectively.

Table 2. FPP of sunspot groups for SC23, SC24, and SC25 based on the third parameter of the modified Zurich classification system

	SC23					SC24			SC25			
	х	0	i	С	х	0	i	С	х	0	i	С
Northern H.	0.04±0.004	0.16±0.005	0.53±0.017	0.76±0.025	0.05±0.006	0.16±0.007	0.39±0.019	0.74±0.024	0.08±0.008	0.27±0.011	0.57±0.022	0.82±0.030
Southern H.	0.04±0.004	0.14±0.005	0.51±0.016	0.67±0.023	0.06±0.006	0.18±0.008	0.45±0.020	0.76±0.019	0.08±0.008	0.28±0.011	0.60±0.019	0.81±0.024

Table 2 shows the FPP of sunspot groups based on the third parameter of the modified Zurich classification system in different hemispheres and cycles. This table confirms the well-established relationship that as the complexity of sunspot groups increases, their FPP also increases. The most pronounced differences in FPP exist in class "c" in SC23 $(0.76\pm0.025 \text{ vs. } 0.67\pm0.023)$, class "i" in SC24 $(0.39\pm0.019 \text{ vs. } 0.45\pm0.020)$, when comparing the northern and southern hemispheres.

Table 3. FER of sunspot groups for SC23, SC24, and SC25 based on the third parameter of the modified Zurich classification system.

		SC23				SC24			SC25				
Г		x	0	i	С	x	0	i	С	х	0	i	С
Г	Northern H.	0.05±0.005	0.28±0.007	1.29±0.039	2.86±0.099	0.09±0.007	0.29±0.010	0.92±0.037	2.88±0.093	0.13±0.011	0.60±0.019	1.74±0.059	3.96±0.155
	Southern H.	0.05±0.005	0.26±0.007	1.27±0.032	2.33±0.070	0.08±0.008	0.35±0.012	1.18±0.042	3.15±0.063	0.12±0.010	0.63±0.017	1.90±0.044	4.19±0.092

Table 3 shows the number density of solar flares produced in different hemispheres and cycles according to the third parameter of the modified Zurich classification system. Although the FER in the classes 'x' and 'o' are similar in both hemispheres, there are differences in the classes 'i' and 'c', especially during SC24 and SC25. In particular, the FER for class "c" in SC25 was calculated as 3.96 ± 0.155 in the northern hemisphere and 4.19 ± 0.092 in the southern hemisphere. This ratio is quite high compared to the other cycles, indicating that the complex sunspot groups in SC25 are more active than the other groups in terms of flare activity.

Table 4 shows the classification of the number of active regions for each hemisphere according to the Z and "c" parameters of the modified Zurich classification. All SSA values are given in millionths of solar hemisphere (μ hem). Based on the study by Kilcik et al. (2011), we classified the A, B, C, H groups as small and the D, E, F groups as large groups in the modified Zurich/McIntosh classification system. Following DeToma et al. (2013) for the analysis for SSA, we have categorized sunspot areas $\leq 100~\mu$ hem (millionths of solar hemisphere) as small and sunspot areas $> 100~\mu$ hem as large. It should be noted that SC23 is stronger in terms of the number of active regions compared to the others and that the southern hemisphere in SC23 is dominant in the entire classification. Several studies have concluded that SC23 was relatively stronger compared to SC24 and SC25 (Kiess et al., 2014; Kakad et al., 2019). The number of sunspots decreased significantly in SC24 compared to SC23, and the occurrence of geomagnetic storms during the ascending phase of SC24 was reported to be lower than in SC23 (Richardson & Cane, 2012).

For large groups (classes D, E, and F according to the modified Zurich classification), as shown in Table 4, f, the southern hemisphere exhibits clear dominance in terms of SSC during SC23, 24, and 25. A similar trend is generally observed in the SSA; however, during SC24, the SSA of both hemispheres are nearly equal. In the case of small groups, the southern hemisphere

Table 4. Total numbers of different parameters across hemispheres and Solar Cycles

	Total Number	Total Number	Total Number	Total Number	Total Number	Total Number
	of S.G. (SSC)	of L.G. (SSC)	of S.G. (SSA)	of L.G. (SSA)	of x and o	of c and i
Northern H.	SC23: 6520	SC23: 3569	SC23: 6972	SC23: 3283	SC23: 9054	SC23: 1201
	SC24: 4257	SC24: 2055	SC24: 4406	SC24: 1891	SC24: 5226	SC24: 1071
	SC25: 1905	SC25: 891	SC25: 1859	SC25: 961	SC25: 2315	SC25: 505
Southern H.	SC23: 6893	SC23: 4446	SC23: 7686	SC23: 3714	SC23: 9861	SC23: 1539
	SC24: 3703	SC24: 2032	SC24: 3898	SC24: 1839	SC24: 4578	SC24: 1159
	SC25: 1933	SC25: 795	SC25: 1782	SC25: 941	SC25: 2295	SC25: 428

158

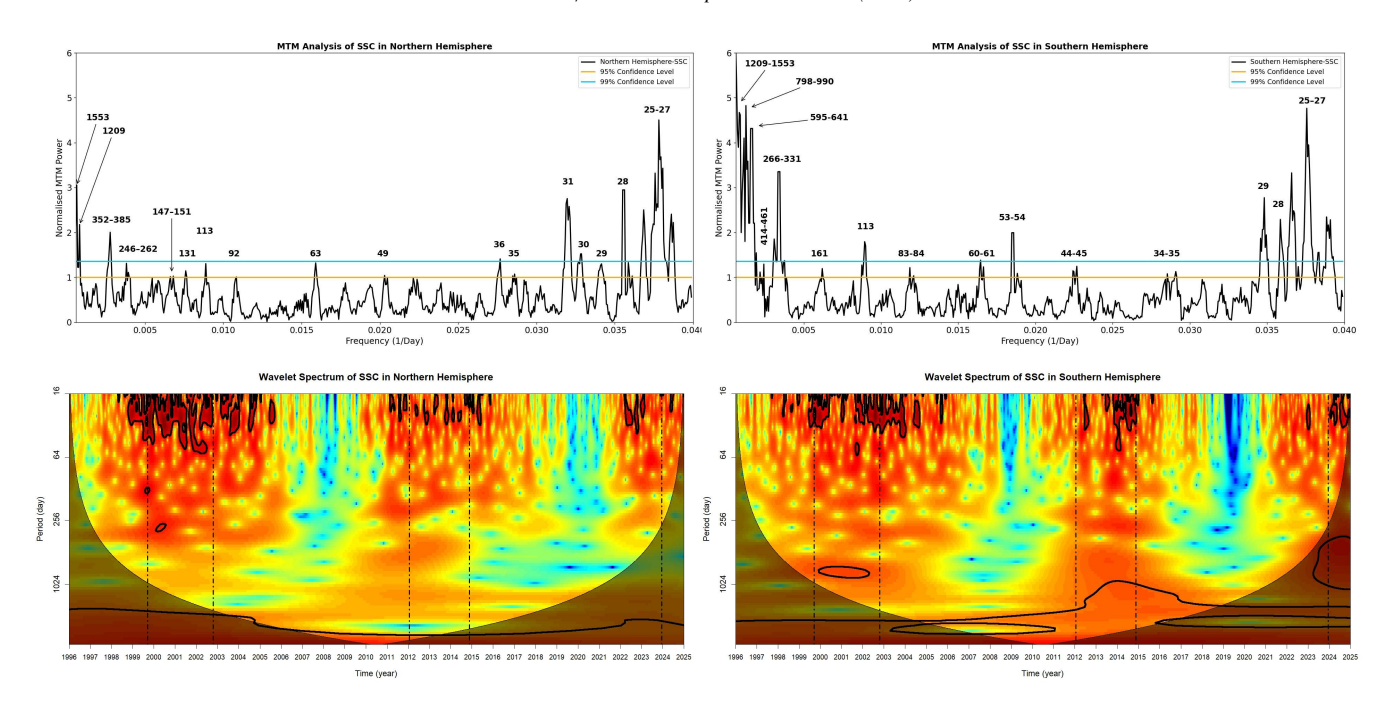


Fig. 2. MTM power spectra (top) and wavelet spectrum (bottom) for SSC (left) in the Northern and Southern Hemispheres (1996–2024). The dashed line in the MTM analysis indicates 95% confidence level and the solid line indicates 99% confidence level. The 95% confidence level in the wavelet spectrum is indicated by the black contours and the cone of influence marked with the shaded area. The intervals of dotted vertical lines mark the maximum phases of SC23, 24, and 25.

generally maintains its dominance, apart from SC24, where the northern hemisphere shows a slightly higher count. However, it is noteworthy that when the sunspot complexity is considered, the number of sunspots with high complexity (classes "c" and "i") for SC23 and SC24 is higher in the southern hemisphere. According to the available data, the southern hemisphere seems to be dominant during SC25. However, a clearer statement is premature, as the data available for the current solar cycle cover only rise up to maximum phase. The cross-correlation analysis revealed correlations coefficients of r = 0.59, r = 0.58, and r = 0.88 between the total number of solar flares and SSA, the total number of solar flares and SSA, respectively.

Figures 2, 3, and 4 illustrate the results of the MTM period analysis and wavelet spectra of SSC, SSA and the total number of x-ray solar flares for the Northern and Southern Hemispheres over the period 1996–2024. The MTM power spectra (top row) highlight significant periodicities exceeding the 95% and 99% confidence levels. The wavelet spectra (bottom row) provide a frequency representation, showcasing the evolution of these periodicities and their dominance during specific solar cycles. To better understand the phase distribution of the periods, the cycle maxima were determined using the SSN $_{\text{limit}} = A - 0.15B$ relationship given by Kilcik and Ozguc (2014), and are indicated by the vertical dotted lines on the graphs. Table 5 lists only significant periods identified via MTM analysis, along with the corresponding solar cycle phases (e.g., ascending, maximum, or descending) in which they were observed. While both MTM and wavelet analyses revealed overlapping periodicities, some were exclusive to one method. This difference likely stems from methodological characteristics: MTM is better suited for stationary signals, whereas wavelets capture localized, transient features and apply smoothing during analysis.

The periodic behaviors of components driving solar activity have revealed several characteristic periods, such as the 27-day solar rotation, the 150-day Rieger periodicity, and quasi-biennial oscillations (QBOs), as well as the long-term 11-year Schwabe cycle. Recent studies indicate that magneto-Rossby waves, which have periods between 0.8 and 2.4 years, significantly contribute to solar variability. Moreover, periodicities ranging from 50 to 130 days and latitudinal oscillations linked to active longitudes have been observed, emphasizing the complex relationship between magnetic and convective processes in the modulation of solar

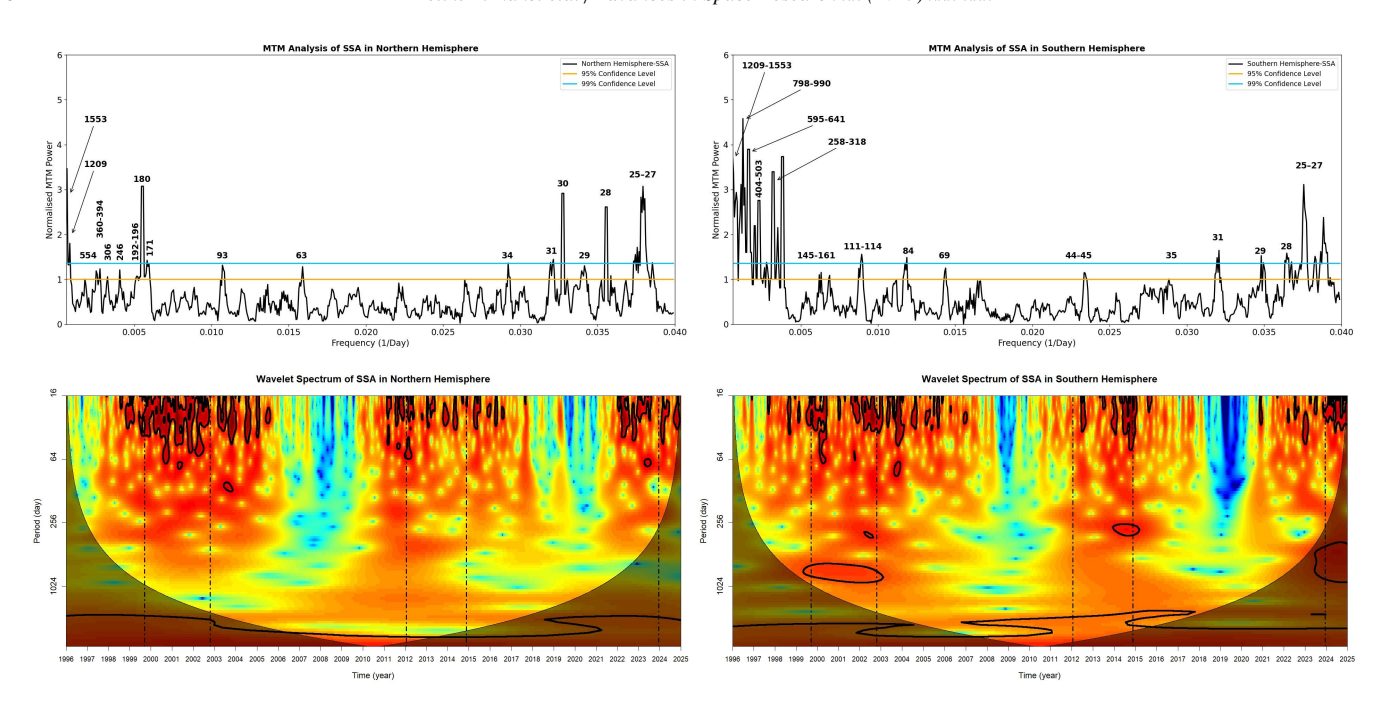


Fig. 3. MTM power spectra (top) and wavelet spectrum (bottom) for SSA in the Northern and Southern Hemispheres (1996-2024).

activity (see Korsós et al., 2023; Elek et al., 2024; Korsós et al., 2024; Wiśniewska et al., 2024). The main periodicities detected in the present study are 25-37 days, 49-63 days, 84-100 days, 254-266 days, and 1126-1553 days. Notably, a 69-day and 595-day periodicity in SSA was observed exclusively in the southern hemisphere during the maximum phase of the solar cycle. In the study by Chowdhury et al. (2009), a period of 69 days was also found and it was stated that the southern hemisphere was more dominant in SC23. The 595-day period falls within the quasi-biennial range (\sim 1.3-2 years) associated with double-peaked solar cycles ((Katsavrias et al., 2012; Hathaway, 2015), suggesting a link to mid-term magnetic modulation processes. The Rieger period of 154 days, first proposed by Rieger et al. (1984) in solar hard-x- and γ -ray flare activity around the maximum phase of SC21, is found as a period in the range of 145-161 days in our study. This periodicity appeared in the North-SSC during the ascending and maximum phases of the cycle, and in the South-Flare during all phases. In addition, the QBOs, sometimes also referred to as intermediate or mid-term quasi-periodicities, are oscillations in the range of 220-1460 days and evolve independently in the solar hemispheres (Bazilevskaya et al., 2014; Kiss et al., 2018; Korsós et al., 2023).

QBOs are observed as ubiquitous in many solar parameters. These groups of periods are also intermittent in nature without stability. The QBO's amplitude follows about 11-year solar cycle, peaking around solar maximum and weakening during the descending/minimum phase (Hathaway, 2015). It was also documented that solar QBOs are transferred into the interplanetary space and reflected in the solar wind, galactic cosmic ray modulation and geophysical disturbances (Wang & Sheeley Jr, 2003; Vecchio & Carbone, 2009; Mursula et al., 2003; Lockwood, 2001, etc.). Studying the nature and evolution of solar QBOs is very important to understand the mechanism behind different solar indices (Hathaway, 2015; Kiss & Erdélyi, 2018). However, it is an interesting finding that the majority of QBOs are found only in the southern hemisphere. Also, we detected a pronounced periodicity of about 5 years in all data sets, which likely shapes the double-peak behavior observed in solar cycles. (Georgieva, 2011). This period is not included in Table 5 as it located outside the COI in the wavelet spectrum. However, such a period was detected in the long-term time series of Ca–K index measured at the Kodaikanal Observatory (Chowdhury et al., 2022).

190

197

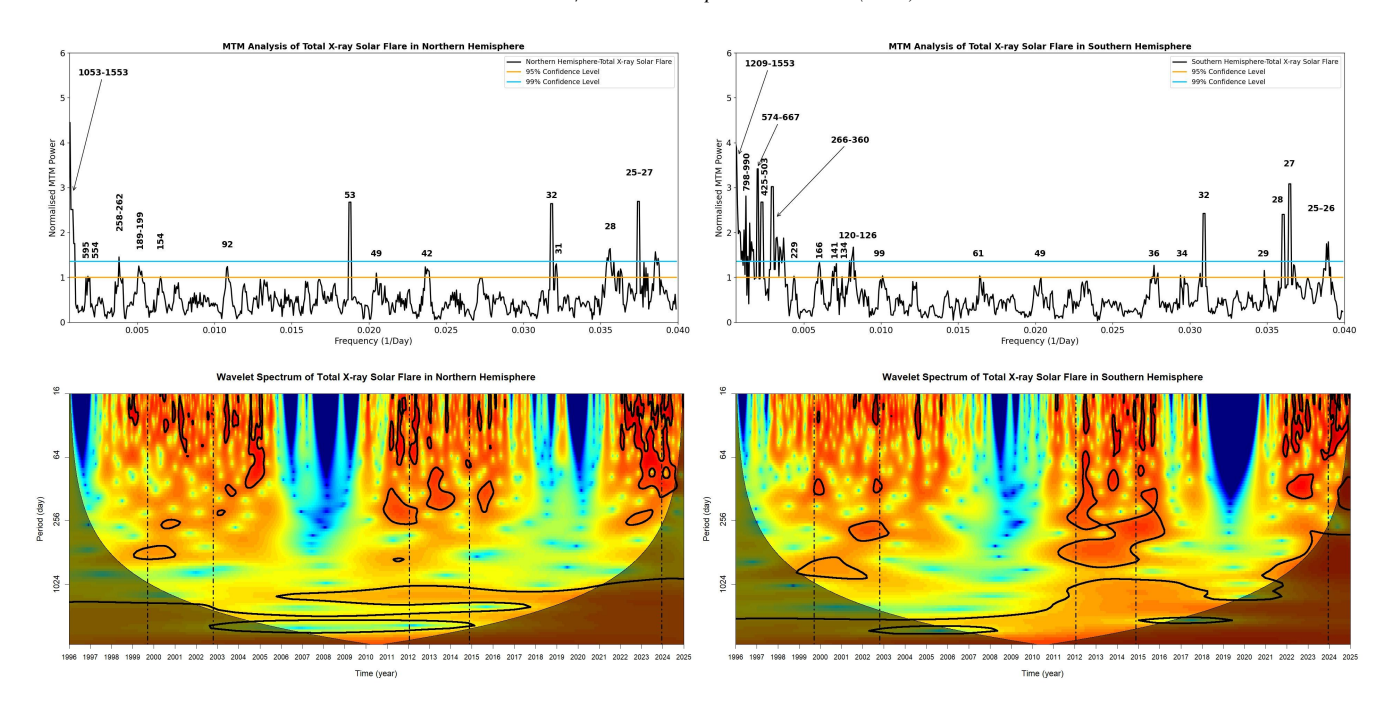


Fig. 4. MTM power spectra (top) and wavelet spectrum (bottom) for total number of x-ray solar flare in the Northern and Southern Hemispheres (1996–2024).

4. Conclusions and Discussions

In this study, the temporal variations of sunspot counts and solar flare numbers are analyzed by taking hemispheric asymmetry into account. Flare production potential of sunspot groups was evaluated by taking into account the intermediate spot distribution. Observed sunspot counts, sunspot areas, and flare numbers show temporal differences based on the asymmetry of the solar hemispheres, together with the investigated cycle. Our main findings are as follows;

- Our findings show that an increase in the complexity of sunspot groups is associated with an increase in FPP and FER. This relationship is consistently observed across different hemispheres and solar cycles. These findings provide further statistical support for using the complexity of sunspot groups as a pre-cursor parameter in models to predict solar flares.
- The number of statistically significant mid-term periods in the northern hemisphere appears to be fewer compared to the southern hemisphere. While QBOs are present in both hemispheres, their spatial and temporal variations manifest unevenly, with the southern hemisphere exhibiting more prominent and distinct evolutionary patterns, particularly during the studied cycles.
- The periodic behaviors of SSC, SSA, and x-ray solar flare numbers exhibit distinct dependencies on the investigated cycle phase and hemispheric asymmetries, with variations in amplitude, shape and timing across different solar cycles.

Our results provides additional insight into the hemispheric asymmetry of solar activity and the interplay among SSC, SSA, solar flares, and sunspot group complexity. The analyses confirm that solar activity exhibits significant hemispheric and temporal variability and confirm well-known trends such as the rotation period, Rieger periods etc.

The hemispheric asymmetry was investigated for many years using various solar activity indices such as sunspot numbers, sunspot areas, solar flares, filaments, coronal mass ejections, etc. (Temmer et al., 2002, 2006; Zhang et al., 2022; Chowdhury et al., 2013; Ataç & Özgüç, 1996; Li et al., 2010; Gao et al., 2009). Typically, hemispheric asymmetry remains below around 20%

Table 5. Detected meaningful MTM periods, their existence, confidence levels, and associated solar cycle phases (A: Ascending, M: Maximum, D: Descending) in each dataset.

Period (Day)	North-SSC	North-SSA	North-Flare	South-SSC	South-SSA	South-Flare
1126–1553	+>99	+>99	+>99	+>99	+>99	+>99
Phase	M-D	M-D	M-D	M-D	M-D	M-D
798–990	_	_	_	+>99	+>99	+>99
Phase	_	_	_	M	M	M
595	_	_	_	+>99	_	_
Phase	_	_	_	M	_	_
503-554	_	+>95	+>95	+>95	+>95	+>99
Phase	_	M-D	M-D	M-D	M-D	M-D
414–461	_	_	_	+>95	+>95	+>95
Phase	_	_	_	M	M	M-D
360–394	+>95	+>95	_	_	+>95	+>95
Phase	_	_	_	_	M	M-D
303–352	_	+>95	+>95	+>95	+>95	+>95
Phase	_	_	M-D	_	M	M-D
246–266	+>95	+>95	+>95	+>95	+>95	_
Phase	M	_	M-D	_	M	_
192–196	+>95	_	_	_	_	_
Phase	A-M	_	_	_	_	_
166–187	_	_	_	_	_	+>95
Phase	_	_	_	_	_	M-D
145–161	+>95	_	_	+>95	+>95	+>95
Phase	A-M	_	_	_	_	A-M-D
111–134	+>95	-	_	+>95	+>95	+>95
Phase	A-M	-	_	_	-	A-M-D
84–100	+>95	_	_	+>95	_	+>95
Phase	A	_	_	A	_	A-D-M
69	_	_	_	+>95	_	_
Phase	_	_	_	M	_	_
49–63	+>95	+>95	+>95	+>95	+>95	+>95
Phase	M	M	A-M-D	M	M	A-M
39–46	_	_	_	+>95	+>95	+>95
Phase	_	_	_	A-M	M	M
25–37	+>95	+>95	+>95	+>95	+>95	+>95
Phase	A	M	M	A	M	M

(Norton et al., 2014). However, during the Maunder Minimum in the late 17th century, nearly all of the few sunspots recorded during this period were concentrated in the southern hemisphere (Vaquero et al., 2015; Schüssler & Cameron, 2018). In our study, the analyses of SSC, SSA and the total number of solar flares during the SC23, SC24 and the ascending and maximum phases of 208 SC25 show a complex relationship between hemispheric dominance and activity patterns. In addition, there is a time lag in the 209 flare times in the northern and southern hemispheres: according to the study by Deng et al. (2017), solar H α flare activity exhibits 210 a strong correlation between both hemispheres, with the northern hemisphere's activity leading that of the southern hemisphere by approximately 7 months. In a similar study by Roy et al. (2020) on solar flare index, the southern hemisphere leads by ten, three and 212 one month during SC21, 22 and 24, respectively. This phase lag suggests a systematic difference in flare timing between the two 213 hemispheres. The temporal relationship between sunspot activity and flare occurrence is not straightforward. For instance, Temmer 214 et al. (2003) studied flare activity in relation to sunspot activity across SC 19-23, identifying a phase lag of about 10-15 months in odd-numbered cycles (19, 21, 23), but no lag was found in even-numbered cycles (20, 22). This aligns with theoretical models by

252

e.g. Wheatland and Litvinenko (2001), who connected flare timing to the transport of magnetic energy from the photosphere to the corona. Later, Feng et al. (2013) used time-frequency analysis to reveal that the phase relationship between solar flares and sunspot numbers varies with both time and frequency, underscoring the nonlinear and complex nature of this interaction.

Based on the temporal variation plots of the SSC and SSA, it is reasonable to say that the solar cycle has gradually weakened since SC23. Many studies have suggested that this phase of decline will continue and SC25 will be weaker compared to SC24, which raises the question 'Will we face a Maunder-like minimum?' (Hathaway & Wilson, 2004; Janardhan et al., 2015; Kakad et al., 2019). Probably one of the most interesting aspects of pronunced N-S asymmetry is that it leads to cycles of lower activity, which can last, as in the case of Maunder Minimum. Although SC25 has not resulted an immediate event similar to the Maunder Minimum, the significant impact of pronounced north-south asymmetry on solar activity is still vital. Several studies indicate that times of strong north-south asymmetry are associated with decreased solar activity and weakened QBOs, which tend to be disrupted during extended low-activity periods (Badalyan & Obridko, 2017; Joshi et al., 2015). This suggests that even though a complete Maunder Minimum scenario has not occurred yet, the noticeable asymmetry and downward trends in solar activity require for further exploration into possible long-term minima. According to the study by Kakad et al. (2019), the integrated solar magnetic energy density decreased by about 37% from SC22 to SC23 and further decreased by 51% from SC23 to SC24 (up to January 2018), indicating a significant weakening of the solar magnetic field during SC24. It has been five years since the beginning of SC25, and a total of 49386 SSCs have been counted. In comparison, during the same period of SC24, the number of recorded SSCs was 37655. These numbers show that SC25 appears to be stronger than SC24; however, earlier studies highlights that both cycles are expected to exhibit comparable amplitudes (Carrasco & Vaquero, 2021; Janssens, 2021; Wu & Qin, 2021). According to Cao et al. (2024), the peak amplitude of SC25 exceeds that of both the preceding SC24 and the following SC26, suggesting that the long-term oscillatory variation of sunspot magnetic fields is linked to the approximately 100-year Gleissberg cycle. While both SSC and SSA increased or remained comparable in the northern hemisphere during SC25 compared to SC24, the southern hemisphere also showed a noticeable increase. The number of observed x-ray flares increased remarkably in both hemispheres during SC25, which may be attributed to the greater presence of complex active regions in the first half of the cycle. Kilcik et al. (2011) concluded that large and complex active regions are observed more frequently during the second half of a cycle, and they may produce more flares. Thus, we may expect more flaring activities in the second half of the current cycle.

SC23 revealed a southern hemisphere dominance in SSC and flare production, and similarly SC24 exhibited a more pronounced southern hemisphere dominance in both metrics. The ongoing SC25 appears to shift the SSC dominance to the northern hemisphere. These findings are consistent with the concept of hemispheric asymmetry in solar activity dominance, but also highlight exceptions, such as the piling up of SSCs and flares in the southern hemisphere of SC24 between 2014 and 2015. This may be explained by the Waldmeier effect, which was outlined by Waldmeier (1935), showing an inverse correlation between the peak amplitude and the rise time of different solar cycles.

The detailed classification of solar flares using the modified Zurich classification system underlines the critical role of sunspot group complexity in flare production. Larger and more complex sunspot groups, particularly those classified as D, E, and F in the modified Zurich system, have a flare production potential approximately eight times higher than simpler groups (A and B classes) (Eren et al., 2017). According to McCloskey et al. (2016), the emergence of magnetic flux in a region produces a greater number of flares compared to the decrease of the flux.

The FPP values in Table 2 indicate that during SC23, SC24, and SC25 the differences in sunspot group complexity between the northern and southern hemispheres were not substantial. Despite some small discrepancies, there are no significant differences

258

259

260

262

263

266

267

268

271

272

273

275

276

277

278

280

281

282

284

285

286

289

290

291

in the FPPs of all complexity groups in both hemispheres. During SC25, the FPP of class "c" increased significantly in both hemispheres compared to previous cycles, reaching 0.82±0.030 in the northern and 0.81±0.024 in the southern hemisphere. This suggests that the probability of flares from the most complex groups during the current cycle is higher. While the FER values in Table 3 for simpler classes ('x' and 'o') remain similar between two hemispheres, notable differences emerge for complex classes ('i' and 'c'), particularly during SC24 and SC25. A striking example is SC25, where the FER for class "c" sunspots reached 3.96±0.155 in the northern and 4.19±0.092 in the southern hemispheres, a significantly higher ratio compared to other cycles. Together, these results highlight the role of sunspot complexity in driving flare activity, though additional factors like magnetic field structure and solar cycle phase may further modulate these activities. It is evident that flare productivity increases in those ARs that exhibit a synchronous increase in both the magnetic helicity and the magnetic flux during their emergence with large changes in sunspot area (Li et al., 2024). Local active regions with intense magnetic flux emergence, such as AR12192 in late 2014, play a disproportionate role in flare production by rapidly injecting helicity and creating highly sheared magnetic structures conducive to reconnection (Sun et al., 2024; Raphaldini et al., 2024). According to Heinemann et al. (2024), AR12192, the largest active region in SC24, produced numerous X-class flares and coincided with the rapid weakening of the remaining southern polar field, emphasizing its influence not only on flare activity but also on the evolution of the large-scale solar magnetic field. This event demonstrates how local magnetic complexity can simultaneously trigger both energetic eruptions and global changes in the solar magnetic environment. This conclusion is supported by our results showing a pronounced hemispheric flare asymmetry in SC24 (-0.12±0.013, from Table 1) and increased flare efficiency of complex sunspot groups in SC25 (from Table 3). This reflects the disproportionate influence of such kind of active regions on solar activity models.

The MTM period analysis adds another layer of complexity to the discussion, identifying several well-known periodicities in solar activity. The detection of the \sim 27-day solar rotation period, Rieger-type periodicities, and quasi-biennial periodicities is consistent with previous studies (Bogard & Bai, 1985; Ozguc & Atac, 1989; Carbonell & Ballester, 1992; Valdés-Galicia & Velasco, 2008; Chowdhury et al., 2009; Kilcik et al., 2016; Korsós et al., 2023; Kilcik et al., 2024). The period of 25-37 days observed in all data is the period of solar rotation and is a result of differential rotation. According to Table 5, this short-term periodicity appears predominantly during the ascending and maximum phases across all datasets, suggesting a strong link to the development and peak phases of solar activity. The other periods found in the study are 49–63, 84–100, 111-134, 145–161, 166–187, 192–196 days. Accordingly, the periods of 111-134, 166-187, 192-196 days that we found in this study are close to the Rieger periodicity, while the period of 145-161 days can be directly attributed to the Rieger periodicity. Note that periods found, such as 49-63, 84–100, 111–134, and 192–196, are probably insignificant because they are multiples of the 27-day solar rotation period. The 145-161-day Rieger-type periodicity was observed with high confidence in the North-SSC dataset during the ascending and maximum phases, and also in South-Flare during all phases (A-M-D), suggesting its cycle-wide significance in both hemispheres. Though the solar dynamo theories successfully explain the ~11-year sunspot cycle to some extent, the origin of several intermediate-term periodicities is not yet fully understood (Charbonneau, 2020, and reference therein). The Rieger group of periods were considered as the nearly integral multiple of the solar rotation periodicity of ~25.1 days according to the clock model proposed by Bai & Sturrock (1993). Some of the observed mid-term periodicities like 129-, 104-, 78- and 51-d were approximately integer multiples of the 25.8 -d periodicity (Bai & Sturrock, 1991), rather than its classical harmonics observed in the Fourier analysis. Ichimoto et al. (1985) conjectured that the 150-160 day periodicity of flare occurrence rate may be considered as the manifestation of a periodic variation of the magnetic field in the solar interior portion. As for the origin of Rieger-type periods, Zaqarashvili et al. (2010) provided a plausible explanation that they are related to the destabilization of magnetic Rossby waves in the solar tachocline due to the joint effect of latitudinal differential rotation and the toroidal magnetic field. Gurgenashvili et al. (2016) studied periodic behavior of sunspot-area data for SC14 to 24 and indicated that the Rieger type of periods are cycle dependent, i.e., shorter periods (150-160 days) occur during stronger solar cycles.

The unstable harmonics of magnetic Rossby waves in this layer cause periodic fluctuations of the magnetic flux at the solar surface, and thus the periodicity is detected in the magnetic activity (Gachechiladze et al., 2019; Xiang et al., 2021). Hanson et al. (2020) reported the signature of these Rossby kinds of waves in the helioseismic data, and McIntosh et al. (2017) observed its evidence in the bright points of the solar corona. So, it is part of a natural process that we encounter these periods in all datasets. Numerical simulations of tachocline fluids by Dikpati et al. (2017; 2018) indicated that MHD Rossby types of waves can create some kinds of nonlinear oscillations in the tachocline region, between their energy and solar differential rotation having periodicity of 6-18 months. These authors argued that these tachocline nonlinear oscillations may generate the "seasons" of the Sun, the profound bursts of solar activities, initiating quieter periods on timescales from 6 to 18 months. Dikpati & McIntosh (2020) composed a list of observational evidence to link the occurrence of the robust solar explosions to magnetic-Rossby types waves in the mid-term period between 8 months and 2.5 yr. Additionally, Korsós et al. (2023), showed that the global solar magnetic field experiences a periodic conveyor belt motion at the equator, along with latitudinal oscillations. Their research revealed that when these movements align with Rieger-type periodicity and magneto-Rossby waves, there is a notable increase in major flare activity, highlighting the key role of Rossby waves in solar activity. A number of investigations indicated the link between the action of magnetic Rossby waves and different solar activities like longitudinal drift of coronal holes (Harris et al., 2022), structure and movement of photospheric magnetic fields (Raphaldini et al., 2023a), recurrent emergence of solar active regions (Raphaldini et al., 2023b; Dikpati et al., 2021), very long-term (few hundreds of years) variations of solar magnetic activities (Zagarashvili et al., 2015; Raphaldini et al., 2020, etc.).

The remaining oscillations, ranging from 246 to 1460 days, fall within the QBO band (Bazilevskaya et al., 2014). A broader low-frequency feature around ~1550 days is also visible, but it lies mostly outside the cone of influence and has a large uncertainty due to its broad peak. Therefore, it is likely consistent with the upper QBO limit rather than representing a distinct periodicity. These longer periodicities are mainly observed during the maximum and descending phases in the southern hemisphere datasets, especially in the southern hemisphere SSA and Flare, indicating a possible hemispheric asymmetry in QBO behavior. Although Frick et al.(2020) argue that no statistically significant mid-term periodicity can be isolated within a continuous turbulent spectrum, our results, based on both MTM and wavelet analyses, clearly reveal consistent periodicities, particularly within the 246-1460 day range, during the maximum and descending phases of the solar cycle. These findings suggest that mid-term oscillations may exhibit temporal phase dependence and are not merely artifacts of stochastic variability. The solar dynamo is thought to be the main mechanism in the formation mechanism of QBOs. The QBOs have been observed from the Sun's subsurface layers (Simoniello et al., 2012, 2013; Jain et al., 2023) to its surface (Benevolenskaya, 1998; Mursula et al., 2003; Vecchio et al., 2012; Kiss et al., 2017, 2018; Kiss & Erdélyi, 2018) and even in neutron counting rates recorded on Earth (Kudela et al., 2010; Chowdhury & Kudela, 2018, etc.). This suggests that QBOs represent a global phenomenon, spanning from the solar interior to Earth through the open solar magnetic field (Inceoglu et al., 2019). In addition, Deng et al. (2020), analyzed the spatial distribution of polar faculae and found that the northern hemisphere exhibited fewer statistically significant mid-term periodicities than the southern hemisphere, as well as marked variations in the occurrence of the OBO, which can be attributed to hemispheric asymmetry. Some solar dynamo models indicate that random fluctuations in the α -effect, particularly when these variations vary by latitude, can trigger QBO that affect the symmetry of solar magnetic activity between two hemispheres. These interactions may explain the reason why QBOs are

335

more evident in the southern hemisphere, as they could reflect deeper asymmetries in the generation and emergence of magnetic flux (Nepomnyashchikh et al., 2019). This finding aligns with our results and we further found similar results three different solar data (SSC, SSA, total number of x-ray flares).

A different perspective highlighting the solar hemispheric asymmetry have been brought here on a cycle-by-cycle basis, leading to better understanding of solar activity.

Acknowledgments

The idea of this study is based on the findings of project 115F031 which was supported by the Scientific and Technical Council of Turkey (TUBITAK). R.E. is grateful to Science and Technology Facilities Council (STFC, grant No. ST/M000826/1) UK, acknowledges NKFIH (OTKA, grant No. K142987 and Excellence Grant, grant nr TKP2021-NKTA-64) Hungary and PIFI (China, grant number No. 2024PVA0043) for enabling this research. This work was also supported by the International Space Science Institute project (ISSI-BJ ID 24-604) on "Small-scale eruptions in the Sun".

References

Akioka, M., Kubota, J., Suzuki, M. et al. (1987). The 17-month periodicity of sunspot activity. Solar Physics, 112(2), 313-316.

Arlt, R., Leussu, R., Giese, N. et al. (2013). Sunspot positions and sizes for 1825–1867 from the observations by samuel heinrich schwabe. *Monthly Notices of the Royal Astronomical Society*, 433(4), 3165–3172.

Ataç, T., & Özgüç, A. (1996). North-south asymmetry in the solar flare index. Solar Physics, 166, 201-208.

Badalyan, O., & Obridko, V. (2017). North-south asymmetry of solar activity as a superposition of two realizations—the sign and absolute value. *Astronomy & Astrophysics*, 603, A109.

Badalyan, O. G., & Obridko, V. N. (2011). North-south asymmetry of the sunspot indices and its quasi-biennial oscillations. New Astronomy, 16(6), 357-365.

Bai, T., & Sturrock, P. A. (1991). The 154-day and related periodicities of solar activity as subharmonics of a fundamental period. *Nature*, 350(6314), 141–143. Bai, T., & Sturrock, P. A. (1993). Evidence for a fundamental period of the sun and its relation to the 154-day complex of periodicities. *Astrophysical Journal*.

Bai, T., & Sturrock, P. A. (1993). Evidence for a fundamental period of the sun and its relation to the 154-day complex of periodicities. *Astrophysical Journal*, 409(1), 476–486.

Bazilevskaya, G., Broomhall, A.-M., Elsworth, Y. et al. (2014). A combined analysis of the observational aspects of the quasi-biennial oscillation in solar magnetic activity. *Space Science Reviews*, 186(1–4), 359–386.

Benevolenskaya, E. E. (1998). A model of the double magnetic cycle of the sun. Astrophysical Journal, 509(1, 2), L49–L52.

Bogard, R. S., & Bai, T. (1985). Confirmation of a 152-day periodicity in the occurrence of solar flares inferred from microwave data. *Astrophysical Journal*, 299(1, 2), L51–L55.

Bornmann, P. L., & Shaw, D. (1994). Flare rates and the mcintosh active-region classifications. Solar Physics, 150(1-2), 127-146.

Cao, J., Xu, T., Deng, L. et al. (2024). Hemispheric prediction of solar cycles 25 and 26 from multivariate sunspot time-series data via informer models. Astronomical Techniques and Instruments, .

Carbonell, M., & Ballester, J. L. (1992). The periodic behavior of solar activity: The near 155-day periodicity in sunspot areas. *Astronomy & Astrophysics*, 255(1–2), 350–362

Carrasco, V., & Vaquero, J. (2021). Solar cycle 25 is currently very similar to solar cycle 24. Research Notes of the AAS, 5(8), 181.

Charbonneau, P. (2020). Dynamo models of the solar cycle. Living Reviews in Solar Physics, 17(1), 4.

Chowdhury, P., Belur, R., Bertello, L. et al. (2022). Analysis of solar hemispheric chromosphere properties using the kodaikanal observatory ca-k index. *The Astrophysical Journal*, 925(1), 81.

Chowdhury, P., Choudhary, D. P., & Gosain, S. (2013). A study of the hemispheric asymmetry of sunspot area during solar cycles 23 and 24. *The Astrophysical Journal*, 768(2), 188.

Chowdhury, P., & Dwivedi, B. N. (2012). Time evolution of short and intermediate term periodicities of electrons at geosynchronous orbit during solar cycle 23 and 24: A wavelet approach. *Planetary and Space Science*, 67(1), 92–100.

Chowdhury, P., Khan, M., & Ray, P. C. (2009). Intermediate-term periodicities in sunspot areas during solar cycles 22 and 23. *Monthly Notices of the Royal Astronomical Society*, 392(3), 1159–1180.

Chowdhury, P., Kilcik, A., Saha, A. et al. (2024). Temporal and periodic analysis of penumbra–umbra ratio for the last four solar cycles. *Solar Physics*, 299(2), 19. Chowdhury, P., Kilcik, A., Yurchyshyn, V. et al. (2019). Analysis of the hemispheric sunspot number time series for the solar cycles 18 to 24. *Solar Physics*, 294, 1–25

Chowdhury, P., & Kudela, K. (2018). Quasi-periodicities in cosmic rays and time lag with the solar activity at a middle latitude neutron monitor: 1982–2017. Astrophysics and Space Science, 363(12), 250.

De Toma, G., Chapman, G. A., Preminger, D. G. et al. (2013). Analysis of sunspot area over two solar cycles. The Astrophysical Journal, 770(2), 89.

Deng, L., Fei, Y., Deng, H. et al. (2020). Spatial distribution of quasi-biennial oscillations in high-latitude solar activity. *Monthly Notices of the Royal Astronomical Society*, 494(4), 4930–4938.

Deng, L., Zhang, X., An, J. et al. (2017). Statistical properties of solar hα flare activity. Journal of Space Weather and Space Climate, 7, A34.

Dikpati, M., Cally, P. S., McIntosh, S. W. et al. (2017). The origin of solar activity periodicities: Analysis using advanced modeling. Scientific Reports, 7, 14750.

Dikpati, M., & McIntosh, S. W. (2020). Solar cycle dynamics: Predictive power using advanced models. Space Weather, 18, e2018SW002109.

Dikpati, M., McIntosh, S. W., Bothun, G. et al. (2018). Long-term solar cycle variations: Data and theoretical models. The Astrophysical Journal, 853, 144.

Dikpati, M., McIntosh, S. W., Chatterjee, S. et al. (2021). Mechanisms behind solar cycle asymmetries: New insights. The Astrophysical Journal, 910, 91.

Elek, A., Korsós, M. B., Dikpati, M. et al. (2024). Exploring spatial and temporal patterns in the debrecen solar faculae database: Part i. *The Astrophysical Journal*, 964(2), 112.

- Emslie, A. G., Dennis, B. R., Shih, A. Y. et al. (2012). Global energetics of thirty-eight large solar eruptive events. Astrophysical Journal, 759(1), 71.
- Erdélyi, R., Korsós, M. B., Huang, X. et al. (2022). The solar activity monitor network–samnet. Journal of Space Weather and Space Climate, 12, Article 2.
- Eren, S., Kilcik, A., Atay, T. et al. (2017). Flare-production potential associated with different sunspot groups. *Monthly Notices of the Royal Astronomical Society*, 465(1), 68–75.
- Farge, M. (1992). Wavelet transforms and their applications to turbulence. Annual Review of Fluid Mechanics, 24(1), 395-458.
- Feng, S., Yu, L., & Yang, Y. (2013). The relationship between grouped solar flares and sunspot activity. *Bulletin of the Astronomical Society in India*, 41, 237–246. Frick, P., Sokoloff, D., Stepanov, R. et al. (2020). Spectral characteristic of mid-term quasi-periodicities in sunspot data. *Monthly Notices of the Royal Astronomical Society*, 491(4), 5572–5578.
- Gachechiladze, T., Zaqarashvili, T. V., Gurgenashvili, E. et al. (2019). Magneto-rossby waves in the solar tachocline and the annual variations in solar activity. *The Astrophysical Journal*, 874(2), 162.
- Gao, P. X. (2020). Curious changes in association of complex sunspot groups with x-ray flares (≥ m1) in solar cycles 22–24. *The Astrophysical Journal*, 894(1), 77. Gao, P. X., Li, K. J., & Shi, X. J. (2009). Hemispheric variation of coronal mass ejections in cycle 23. *Monthly Notices of the Royal Astronomical Society*, 400(3), 1383–1388
- Georgieva, K. (2011). Why the sunspot cycle is double peaked. International Scholarly Research Notices, 2011(1), 437838.
- Georgieva, K., & Veretenenko, S. (2023). Solar influences on the earth's atmosphere: solved and unsolved questions. *Frontiers in Astronomy and Space Sciences*, 10, 1244402.
- Georgoulis, M. K., Yardley, S. L., Guerra, J. A. et al. (2024). Prediction of solar energetic events impacting space weather conditions. Advances in Space Research,
- Ghil, M., Allen, M. R., Dettinger, M. D. et al. (2002). Advanced spectral methods for climatic time series. Reviews of Geophysics, 40(1), 1003.
- Gurgenashvili, E., Zaqarashvili, T. V., Kukhianidze, V. et al. (2016). Rieger-type periodicity during solar cycles 14–24: Estimation of dynamo magnetic field strength in the solar interior. *Astrophysical Journal*, 826(1), 55.
- Hanson, C. S., Gizon, L., & Liang, Z. C. (2020). Solar rossby waves observed in gong++ ring-diagram flow maps. Astronomy & Astrophysics, 635, A109.
- Harris, J., Dikpati, M., Hewins, I. M. et al. (2022). Advances in solar cycle analysis: Rossby wave dynamics. The Astrophysical Journal, 931, 54.
- Hathaway, D. H. (2015). The solar cycle. Living Reviews in Solar Physics, 12(1), 4.
- Hathaway, D. H., & Wilson, R. M. (2004). What the sunspot record tells us about space climate. Solar Physics, 224(1), 5-19.
- Heinemann, S. G., Owens, M. J., Temmer, M. et al. (2024). On the origin of the sudden heliospheric open magnetic flux enhancement during the 2014 pole reversal. The Astrophysical Journal, 965(2), 151.
- Ichimoto, K., Kubota, J., Suzuki, M. et al. (1985). Periodic behaviour of solar flare activity. Nature, 316(6027), 422-424.
- Inceoglu, F., Simoniello, R., Arlt, R. et al. (2019). Constraining non-linear dynamo models using quasi-biennial oscillations from sunspot area data. *Astronomy & Astrophysics*, 625, A117.
- Jain, K., Chowdhury, P., & Tripathy, S. C. (2023). Helioseismic investigation of quasi-biennial oscillation source regions. *The Astrophysical Journal*, 959(1), 16.
 Janardhan, P., Bisoi, S. K., Ananthakrishnan, S. et al. (2015). A 20 year decline in solar photospheric magnetic fields: Inner-heliospheric signatures and possible implications. *Journal of Geophysical Research: Space Physics*, 120(7), 5306–5317.
- Janssens, J. (2021). Prediction of the amplitude of solar cycle 25 using polar faculae observations. Journal of Space Weather and Space Climate, 11, 3.
- Janssens, J., Delouille, V., Clette, F. et al. (2025). Solar flare rates and probabilities based on the mcintosh classification: Impacts of goes/xrs rescaling and revisited sunspot classifications. *Journal of Space Weather and Space Climate*, 15, 14.
- Joshi, B., Bhattacharyya, R., Pandey, K. et al. (2015). Evolutionary aspects and north-south asymmetry of soft x-ray flare index during solar cycles 21, 22, and 23. Astronomy & Astrophysics, 582, A4.
- Kakad, B., Kakad, A., Ramesh, D. S. et al. (2019). Diminishing activity of recent solar cycles (22–24) and their impact on geospace. *Journal of Space Weather and Space Climate*, 9, A1.
- Katsavrias, C., Preka-Papadema, P., & Moussas, X. (2012). Wavelet analysis on solar wind parameters and geomagnetic indices. Solar Physics, 280, 623-640.
- Kiess, C., Rezaei, R., & Schmidt, W. (2014). Comparison of sunspot properties in cycle 24 and 23. HMI Science Nuggets, .
- Kilcik, A., Chowdhury, P., Sarp, V. et al. (2020). Temporal and periodic variation of the memesi for the last two solar cycles; comparison with the number of different class x-ray solar flares. *Solar Physics*, 295, 1–17.
- Kilcik, A., & Ozguc, A. (2014). One possible reason for double-peaked maxima in solar cycles: is a second maximum of solar cycle 24 expected? *Solar Physics*, 289(4), 1379–1386.
- Kilcik, A., Rozelot, J. P., & Ozguc, A. (2024). Periodic behavior of selected solar, geomagnetic and cosmic activity indices during solar cycle 24. *Universe*, 10(3), 107
- Kilcik, A., Yurchyshyn, V., Clette, F. et al. (2016). Active latitude oscillations observed on the sun. Solar Physics, 291, 1077-1087.
- Kilcik, A., Yurchyshyn, V., Donmez, B. et al. (2018). Temporal and periodic variations of sunspot counts in flaring and non-flaring active regions. *Solar Physics*, 293(4), 63.
- Kilcik, A., Yurchyshyn, V. B., Abramenko, V. et al. (2011). Time distributions of large and small sunspot groups over four solar cycles. *The Astrophysical Journal*, 731(1), 30.
- Kiss, T. S., & Erdélyi, R. (2018). On quasi-biennial oscillations in chromospheric macrospicules and their potential relation to the global solar magnetic field. *The Astrophysical Journal*, 857(2), 113.
- Kiss, T. S., Gyenge, N., & Erdélyi, R. (2017). Systematic variations of macrospicule properties observed by sdo/aia over half a decade. *The Astrophysical Journal*, 835(1), 47.
- Kiss, T. S., Gyenge, N., & Erdélyi, R. (2018). Quasi-biennial oscillations in the cross-correlation of properties of macrospicules. *Advances in Space Research*, 61(2), 611–616.
- Knaack, R., Stenflo, J. O., & Berdyugina, S. V. (2005). Evolution and rotation of large-scale photospheric magnetic fields of the sun during cycles 21–23-periodicities, north-south asymmetries and r-mode signatures. *Astronomy & Astrophysics*, 438(3), 1067–1082.
- Korsós, M. B., Dikpati, M., Erdélyi, R. et al. (2023). On the connection between rieger-type and magneto-rossby waves driving the frequency of the large solar eruptions during solar cycles 19–25. *The Astrophysical Journal*, 944(2), 180.
- Korsós, M. B., Georgoulis, M. K., Gyenge, N. et al. (2020). Solar flare prediction using magnetic field diagnostics above the photosphere. *The Astrophysical Journal*, 896(2), 119.
- Korsós, M. B., Jarolim, R., Erdélyi, R. et al. (2024). First insights into the applicability and importance of different 3d magnetic field extrapolation approaches for studying the preeruptive conditions of solar active regions. *The Astrophysical Journal*, 962(2), 171.
- Korsós, M. B., Ludmány, A., Erdélyi, R. et al. (2015). On flare predictability based on sunspot group evolution. The Astrophysical Journal Letters, 802(2), L21.
- Kudela, K., Mavromichalaki, H., Papaioannou, A. et al. (2010). On mid-term periodicities in cosmic rays. Solar Physics, 266, 173–180.
- Lau, K. M., & Weng, H. (1995). Climate signal detection using wavelet transform: How to make a time series sing. *Bulletin of the American Meteorological Society*, 76(12), 2391–2402.

Lean, J. L., & Brueckner, G. E. (1989). Intermediate-term solar periodicities: 100-500 days. Astrophysical Journal, 337(1), 568-578.

Li, F., Rao, C., Wang, H. et al. (2024). Large eruptive and confined flares in relation to the solar active region evolution. *The Astrophysical Journal Letters*, 976(1), L.2.

Li, K., Chen, H., Zhan, L. et al. (2009). Asymmetry of solar activity in cycle 23. Journal of Geophysical Research: Space Physics, 114(A4).

Li, K. J., Liu, X. H., Gao, P. X. et al. (2010). The north-south asymmetry of filaments in solar cycles 16-21. New Astronomy, 15(4), 346-350.

Lin, J., Wang, F., Deng, L. et al. (2023). Evolutionary relationship between sunspot groups and soft x-ray flares over solar cycles 21–25. *The Astrophysical Journal*, 958(1), 1.

Lockwood, M. (2001). Long-term variations in the magnetic fields of the sun and the heliosphere: Their origin, effects, and implications. *Journal of Geophysical Research: Space Physics*, 106(A8), 16021–16038.

McCloskey, A. E., Gallagher, P. T., & Bloomfield, D. S. (2016). Flaring rates and the evolution of sunspot group meintosh classifications. *Solar Physics*, 291(6), 1711–1738.

McIntosh, P. S. (1990). The classification of sunspot groups. Solar Physics, 125, 251–267.

McIntosh, S. W., Cramer, W. J., Pichardo Marcano, M. et al. (2017). The detection of rossby-like waves on the sun. Nature Astronomy, 1(4), 0086.

McIntosh, S. W., Leamon, R. J., Krista, L. D. et al. (2015). The solar magnetic activity band interaction and instabilities that shape quasi-periodic variability. *Nature Communications*, 6, 6491.

Mursula, K., Zieger, B., & Vilppola, J. H. (2003). Mid-term quasi-periodicities in geomagnetic activity during the last 15 solar cycles: Connection to solar dynamo strength. *Solar Physics*, 212, 201–207.

Nepomnyashchikh, A., Mandal, S., Banerjee, D. et al. (2019). Can the long-term hemispheric asymmetry of solar activity result from fluctuations in dynamo parameters? *Astronomy & Astrophysics*, 625, A37.

Norton, A. A., Gilman, P. A., & Howard, R. F. (2014). North-south asymmetry of solar activity as a superposition of two dynamo modes. *Astronomy & Astrophysics*, 603, A109.

Obridko, V. N., & Shelting, B. D. (2001). Quasi-biennial oscillations of the global solar magnetic field. Astronomy Reports, 45, 1012-1017.

Oliver, R., Ballester, J. L., & Baudin, F. (1998). Emergence of magnetic flux on the sun as the cause of a 158-day periodicity in sunspot areas. *Nature*, 394(6693), 552–553.

Oloketuyi, J., Liu, Y., & Elmhamdi, A. (2023). Investigating the associations between solar flares and magnetic complexity of active regions. *New Astronomy*, 100, 101972

Ozguc, A., & Atac, T. (1989). Periodic behavior of solar flare index during solar cycles 20 and 21. Solar Physics, 123, 357-365.

Park, J. (1992). Envelope estimation for quasi-periodic geophysical signals in noise: a multitaper approach. *Statistics in the Environmental and Earth Sciences, Arnold, London*, (p. 189).

Priest, E. R., & Forbes, T. G. (2002). The magnetic nature of solar flares. The Astronomy and Astrophysics Review, 10(4), 313–377.

Pulkkinen, T. (2007). Space weather: Terrestrial perspective. Living Reviews in Solar Physics, 4(1), 1.

Raphaldini, B., Dikpati, M., McIntosh, S. W. et al. (2023a). Solar magnetic dynamics and implications for solar cycles. The Astrophysical Journal, 953, 156.

Raphaldini, B., Dikpati, M., Norton, A. A. et al. (2023b). Analysis of magnetohydrodynamic processes in solar cycles. The Astrophysical Journal, 958, 175.

Raphaldini, B., Dikpati, M., Teruya, A. et al. (2024). Global and local dynamics of x-flare-producing active regions during solar cycle 25 peak phase. *Astronomy & Astrophysics*, 691, A3.

Raphaldini, B., Medeiros, E., Raupp, C. F. et al. (2020). Advances in solar dynamo modeling: A new perspective. The Astrophysical Journal, 890, L13.

Ravindra, B., Chowdhury, P., & Javaraiah, J. (2021). Solar-cycle characteristics in kodaikanal sunspot area: North–south asymmetry, phase distribution and gnevyshev gap. Solar Physics, 296(1), 2.

Ravindra, B., Chowdhury, P., Ray, P. C. et al. (2022). Temporal evolutions and quasiperiodic variations present in the sunspot number and group sunspot area data measured at kodaikanal observatory for solar cycles 14–24. *The Astrophysical Journal*, 940(1), 43.

Richardson, I. G., & Cane, H. V. (2012). Near-earth solar wind flows and related geomagnetic activity during more than four solar cycles (1963–2011). *Journal of Space Weather and Space Climate*, 2, A02.

Rieger, E., Share, G. H., Forrest, D. J. et al. (1984). A 154-day periodicity in the occurrence of hard solar flares? Nature, 312(5995), 623-625.

Roy, S., Prasad, A., Ghosh, K. et al. (2020). Investigation of the hemispheric asymmetry in solar flare index during solar cycle 21–24 from the kandilli observatory. *Solar Physics*, 295, 1–22.

Sammis, I., Tang, F., & Zirin, H. (2000). The dependence of large flare occurrence on the magnetic structure of sunspots. *The Astrophysical Journal*, 540(1), 583. Schrijver, C. J., & Mitchell, S. D. (2013). Disturbances in the us electric grid associated with geomagnetic activity. *Journal of Space Weather and Space Climate*, 3, A19.

Schüssler, M., & Cameron, R. H. (2018). Origin of the hemispheric asymmetry of solar activity. Astronomy & Astrophysics, 618, A89.

Schüssler, M., & Cameron, R. H. (2018). The solar cycle and the north-south asymmetry of solar activity. Astronomy & Astrophysics, 615, A1.

Shibata, K., & Magara, T. (2011). Solar flares: magnetohydrodynamic processes. Living Reviews in Solar Physics, 8(1), 1–99.

Simoniello, R., Finsterle, W., Salabert, D. et al. (2012). The quasi-biennial periodicity (qbp) in velocity and intensity helioseismic observations-the seismic qbp over solar cycle 23. Astronomy & Astrophysics, 539, A135.

Simoniello, R., Jain, K., Tripathy, S. C. et al. (2013). The quasi-biennial periodicity as a window on the solar magnetic dynamo configuration. *The Astrophysical Journal*, 765(2), 100.

Smith, S. F., & Howard, R. F. (1968). Iau symp. 35, 33, .

Sun, Z., Li, T., Wang, Q. et al. (2024). Magnetic helicity evolution during active region emergence and subsequent flare productivity. *Astronomy & Astrophysics*, 686, A148.

Tellinghuisen, J. (2001). Statistical error propagation. The Journal of Physical Chemistry A, 105(15), 3917–3921.

Temmer, M. (2021). Space weather: The solar perspective: An update to schwenn (2006). Living Reviews in Solar Physics, 18(1), 4.

Temmer, M., Rybák, J., Bendík, P. et al. (2006). Hemispheric sunspot numbers rn and rs from 1945-2004: Catalogue and n-s asymmetry analysis for solar cycles 18-23. Astronomy & Astrophysics, 447(2), 735–743.

Temmer, M., Veronig, A., & Hanslmeier, A. (2002). Hemispheric sunspot numbers and: Catalogue and ns asymmetry analysis. *Astronomy & Astrophysics*, 390(2), 707–715.

Temmer, M., Veronig, A., & Hanslmeier, A. (2003). Does solar flare activity lag behind sunspot activity? Solar Physics, 215, 111–126.

Thomson, D. J. (1982). Spectrum estimation and harmonic analysis. Proc. IEEE, 70, 1055.

Toriumi, S., Schrijver, C. J., Harra, L. K. et al. (2017). Magnetic properties of solar active regions that govern large solar flares and eruptions. *The Astrophysical Journal*, 834(1), 56.

Toriumi, S., & Wang, H. (2019). Flare-productive active regions. Living Reviews in Solar Physics, 16(1), 3.

Torrence, C., & Compo, G. P. (1998). A practical guide to wavelet analysis. Bulletin of the American Meteorological Society, 79(1), 61-78.

Usoskin, I. G. (2017). A history of solar activity over millennia. Living Reviews in Solar Physics, 14(1), 3.

Valdés-Galicia, J. F., & Velasco, V. M. (2008). Variations of mid-term periodicities in solar activity physical phenomena. Advances in Space Research, 41(2), 297–305

Vaquero, J. M., Nogales, J. M., & Sánchez-Bajo, F. (2015). Sunspot latitudes during the maunder minimum: A machine-readable catalogue from previous studies. Advances in Space Research, 55(6), 1546–1552.

Vecchio, A., & Carbone, V. (2009). Spatio-temporal analysis of solar activity: main periodicities and period length variations. *Astronomy & Astrophysics*, 502(3), 981–987.

Vecchio, A., Laurenza, M., Meduri, D. et al. (2012). The dynamics of the solar magnetic field: polarity reversals, butterfly diagram, and quasi-biennial oscillations. The Astrophysical Journal, 749(1), 27.

Waldmeier, M. (1935). Astron. mitt. eidgen. sternw. zürich, 14, 105, .

Wang, Y.-M., & Sheeley Jr, N. (2003). On the fluctuating component of the sun's large-scale magnetic field. The Astrophysical Journal, 590(2), 1111.

Wheatland, M., & Litvinenko, Y. E. (2001). Energy balance in the flaring solar corona. The Astrophysical Journal, 557(1), 332.

Wiśniewska, A., Korsós, M., Kontogiannis, I. et al. (2024). Long-period oscillations in the lower solar atmosphere prior to flare events. *Astronomy & Astrophysics*, 686, A224.

Wu, S.-S., & Qin, G. (2021). Predicting sunspot numbers for solar cycles 25 and 26. arXiv preprint arXiv:2102.06001, .

Xiang, N. B., Zhao, X. H., & Li, F. Y. (2021). The cause of the appearance or disappearance of the rieger-type periodicity in the northern and southern hemispheres of the sun. *Publications of the Astronomical Society of Australia*, 38, e032.

Zaqarashvili, T. V., Carbonell, M., Oliver, R. et al. (2010). Magnetic rossby waves in the solar tachocline and rieger-type periodicities. *The Astrophysical Journal*, 709(2), 749.

Zaqarashvili, T. V., Oliver, R., Hanslmeier, A. et al. (2015). Magnetic rossby wave dynamics and solar cycle periodicities. *The Astrophysical Journal*, 805, L14.

Zhang, L., Mursula, K., & Usoskin, I. (2015). Solar surface rotation: Ns asymmetry and recent speed-up. Astronomy & Astrophysics, 575, L2.

Zhang, X. J., Deng, L. H., Fei, Y. et al. (2022). Hemispheric asymmetry of long-term sunspot activity: sunspot relative numbers for 1939–2019. *Monthly Notices of the Royal Astronomical Society*, 514(1), 1140–1147.

Zirin, H., & Liggett, M. A. (1987). Delta spots and great flares. Solar Physics, 113, 267-283.